ANALYSIS OF SWIRL TUBE AS DOWNHOLE DESANDER DEVICE

Jason Alves Martins
Eugênio Spanó Rosa
Energy Dept. – FEM – State University of Campinas
jamartins@fem.unicamp.br & erosa@fem.unicamp.br

Abstract. *This work investigates the solid-liquid separation mechanisms in swirl-tubes. One seeks to disclose the flow features leading to the solid separation or not. The flow field is solved in a structured grid using a finite volume method. Capture surfaces are drawn inside the domain based on the solid terminal velocity and the flow field velocities. The capture surface is a threshold surface; once the solids cross a capture surface they are no-longer separated by the device. A reference case is established and a comparative analysis of the flow field and capture surfaces are developed against cases where the liquid flow rate or the particle diameter or the liquid viscosity varies. The separation trend revealed by the numerical analysis is consistent with the experimentally determined solids separation efficiency.*

Keywords: *Swirl Tube, Separation, Solid-Liquid, Finite Volume Method.*

1. Introduction

Swirl tubes are often employed by the oil industry as a desander device for crude production in land fields with high water cut (95% to 99%). With reduced size and no moving parts these devices are fitted to work at the bottom of the well separating the sand from the upstream liquid flow. They reduce the well workover and servicing activities by avoiding sand to reach the pumping system and other pipeline accessories. The swirl tubes are usually installed in vertical or near vertical well bores above the oil formation; Fig. 1(a) depicts the application scenario. The device consists of two concentric pipes which overlap each other forming a chicane, Fig. 1(b). Within the annular space between the pipes there are no-moving vanes to impart a swirl component on the downward liquid stream. At the chicane the liquid stream is diverted upward toward the production line while the solids proceed downstream on the external pipe to the solids reservoir. These separation devices deals with solids concentration typically less than 0.1% and are best fit for continuous operation rather than to slug flow. They handle liquid flow rates from low to moderate range, 20 m^3/d to 600 m^3/d. The gas content is typically limited to 2% in volume at operation condition. Eventually higher gas contents can be handled with increase in size of the equipment. Applications with heavy crude or oil-water mixtures with lower water cuts are not successfully reported. The drop on the separation efficiency or even its complete failure is attributed to the increase of the liquid viscosity due to the formation of oil-water emulsion.

At the moment is not known the impact of the liquid viscosity increase on the separation efficiency of the swirl tubes. An experimental test campaign, taken at the flow laboratory of the Energy department, investigated how the liquid viscosity increase changes the separation efficiency. The tests reproduced the field scenario and employed a 1:1 scale swirl tube with dimensions shown in Fig. 1(b). The test fluid was a water-glycerin solution with various concentrations such that the liquid viscosity was allowed to change from 1cP up to 100cP. The solids were glass spheres with diameter of 250μm, 900μm and 4000μm. The experimental tests revealed that the separation efficiency increases as the liquid viscosity decreases or the liquid flow rate increase or the particle size increase. The experimental results were reduced to a single relationship involving dimensionless parameters which accurately described the separation efficiency; see Martins and Rosa (2005).

Even though the separation efficiency has its behavior described by an algebraic equation involving dimensionless groups it does not describe the flow mechanisms responsible for increasing or decreasing the separation efficiency. To gain insight to design theses devices to handle more viscous liquids is necessary to understand the physics of the solid-liquid separation in regard to the operational and geometrical parameters of the device. This paper adds on the experimental work of Martins and Rosa (2005) addressing, from a qualitatively point of view, what are the flow mechanism underlining the separation efficiency. The paper is organized as follow. The numerical method, grid size, convergence criteria and boundary conditions are described in section 2. The flow field analysis is done in section 3. The concept of the capture surface and time of residence are introduced at section 4. Section 5 does a comparative study of three cases where the liquid flow rate, the liquid viscosity and particle diameter changes. Finally some conclusions are drawn in section 6.

2. Numerical Method

This section presents the numerical method and describes the grid size, boundary conditions and the convergence criterion. The mass and momentum equations are solved using the finite volume technique (Patankar, 1980) embodied on the Phoenics 3.5.1 cfd code. The flow is considered to be in steady state, incompressible and axis-symmetric. A structured cylindrical polar grid properly describes the flow domain inside the swirl tube. The orthogonal directions are

X, Y and Z representing the tangential, radial and axial directions respectively. The flow field has three velocity components: U, V and W, which correspond to the velocities along the X, Y and Z directions.

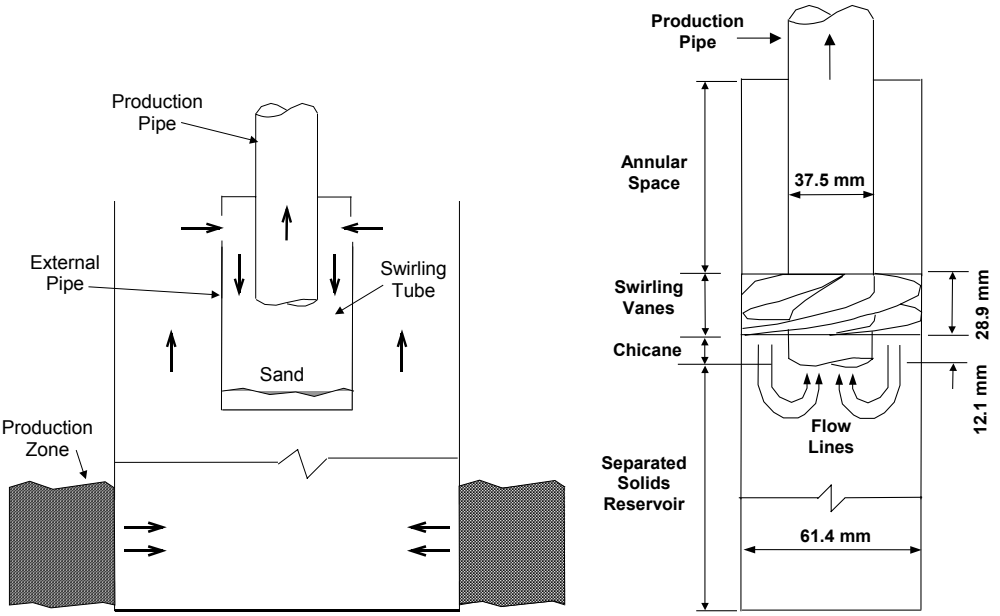

(a) (b)

Figure 1. (a) Schematic of swirl tube inside the well and (b) swirl tube main dimensions.

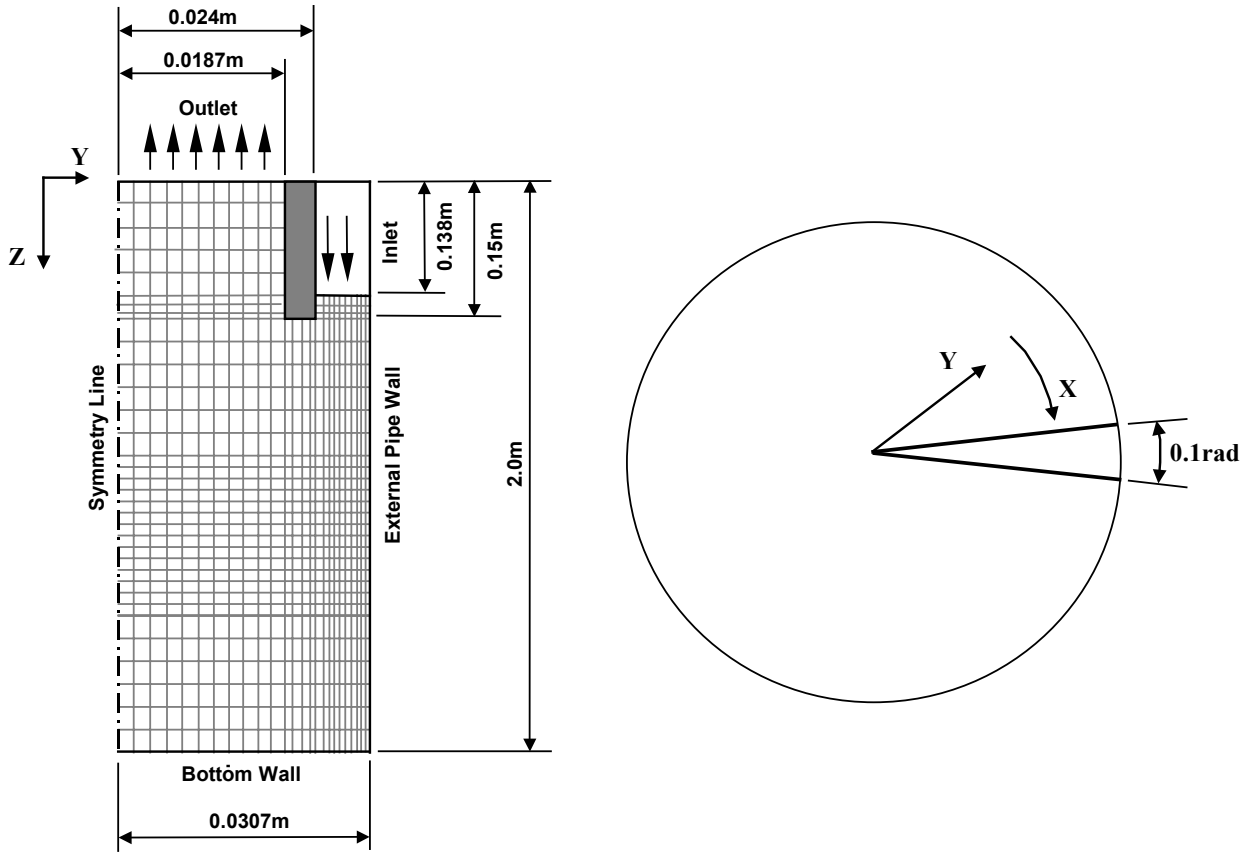

(a) (b)

Figure 2. Schematic of the grid

The domain size along the X, Y and Z directions are, respectively, 0.1 rad, 0.0307 m and 2.0 m. The structured orthogonal grid is non-uniform along the Y and Z directions. The grid knots density is proportional to the flow gradients, the steeper the gradients the denser is the grid. The influence of the grid size on the numerical outputs is accessed using three grids, each one having 1x13x70, 1x25x141 and 1x50x282 corresponding to the number of control volumes along the X, Y and Z. There are changes between the first and the second grid but from the second to the third they are quite small indicating numerical convergence. This work employs a grid with 1x25x141 to better compromise between computer time and numerical accuracy.

The boundary conditions used in this work are: mass and momentum inflow at the inlet, no-slip at the external and bottom walls, periodic flow along X direction, flow symmetry at the centerline and at the outlet the flow is locally parabolic. For reference they are schematically represented in Fig. 2. The inlet is placed at $0.024 < Y < 0.0307$ and $Z = 0.138$ m. At the inlet are specified the axial and swirl inlet velocities: Win and Uin, which bear the relationship: $\tan(\alpha) = Win/Uin$, where α is the angle that the stationary blade makes with the horizontal line, $\alpha = 0.175$ rad. The no-slip is enforced at the external wall, at the bottom wall and at the blockage between the inlet and outlet. Tangential symmetry is enforced applying a periodic condition along X direction. At the symmetry line, $Y = 0$ and $0 < Z < 2$ all variables gradients are null. The outlet is at $0 < Y < 0.0187$ and $Z = 0$, the diffusion coefficients are null and the pressure is let to float along Y accordingly to the resultant centrifugal force field.

The numerical solution stopped when the sum, over all control volumes, of the residuals of the mass and the momentum equations falls below 0.2% of the reference mass and momentum fluxes. The reference fluxes for the X and Z directions are taken as the mass and momentum fluxes happening at the inlet. For convenience, the reference momentum flux for the Y direction was also taken as equal to the reference momentum flux for the Z direction.

3. Flow field analysis

The flow field inside the swirl tube has the axial, radial and tangential velocities, W, V and U respectively. The interplay of these three components rules the solid particle trajectory and defines if it will be separated or not. The analysis starts with a reference case defined by: liquid flow rate of 116 m^3/d, liquid viscosity of 20 cP and swirl angle of 10 degrees. The contours of swirl velocity, the axial velocity and the streamlines for the reference case are displayed in Fig. 3. Exploring the axis-symmetry they show the contours from the center line until the outer wall, the figure dimension is not in scale but magnified 10 times along the radial direction. The swirl velocity is maximum (6.5 m/s) at the inlet and decays along the axial direction as well as when it approaches the center of the tube. The axial velocity describes a U turn inside the device since its bottom is closed and the outlet, i.e. the production tube, is placed almost side by side with the inlet area. The axial W velocities have positive and negative values representing the downward and upward directions respectively. The maximum downward velocity is of 1.5 m/s at the inlet region and the minimum upward velocity is of -2 m/s near the production pipe inlet. Along any cross section the W velocity shows decay in absolute value as the z coordinate increases. The streamlines are at the right of Fig. 3 and disclose that the liquid makes the U turn progressively. The streamlines starting at the inner region of the inlet are the first to turn and travel a short distance along the axial direction before exiting the domain. On the other hand, the streamlines starting at the outer region of the inlet have to travel a greater axial distance and are the last to turn upward. The streamline pattern also discloses that radial velocity field always point toward the tube centerline.

The rate of decay of the swirl and axial velocity along the z axis are more accurately represented by the x-y plot in Fig. 4 taken at four axial positions downstream the inlet: 161mm, 500mm, 1000mm and 1400mm. These axial positions are represented as external marks along the streamlines pattern in Fig. 3 for reference. Considering Fig. 4(a) at a given section z, U is near zero at the tube centerline, grows almost linearly as the y coordinate increases, reach a maximum near the inlet region and falls to zero again due to the no-slip condition. The quasi-linear growth rate of U near the tube centerline indicates that the fluid rotates like a rigid body. Keeping constant the y coordinate one sees that the U velocity always decays as the axial position increases. There is no significant swirl velocity 1400 mm downstream the inlet. The axial velocity profile at distinct z sections are in Fig. 4(b). The axial velocity near the tube centerline has a minimum, grows monotonically, crosses the zero value, reaches a maximum at the inlet region and then falls to zero again near at the pipe wall. The radial distance where the W is zero is near the same for all other z sections, $y = 0.022$ m, coincident with the outer diameter of the production tube. The absolute value of W decays with downstream from the inlet, at 1400 mm downstream the inlet W is near zero.

In order to the liquid do a U turn inside the device is necessary that the downward liquid stream be progressively reduced transferring liquid to the upward stream. The downward liquid flow rate, defined as Qz, is determined summing the product of the cell areas times the *positive* W velocity component along any z section. Of course the upward liquid flow rate has the same magnitude of Qz but opposite sign to conserve mass. Qz is proportional to the average downward W velocity and is useful to disclose its decaying rate. Figure 5(a) displays the ratio Qz/Q for the reference case against two other cases, as shown in Tab. 1. The first pair has the same liquid flow rate but liquid viscosities of 20cP and 100cP. The second pair keeps the same liquid viscosity of 20cP but reduces the liquid flow rate from116m^3/d to 60 m^3/d. In all cases the swirl angle is kept the same.

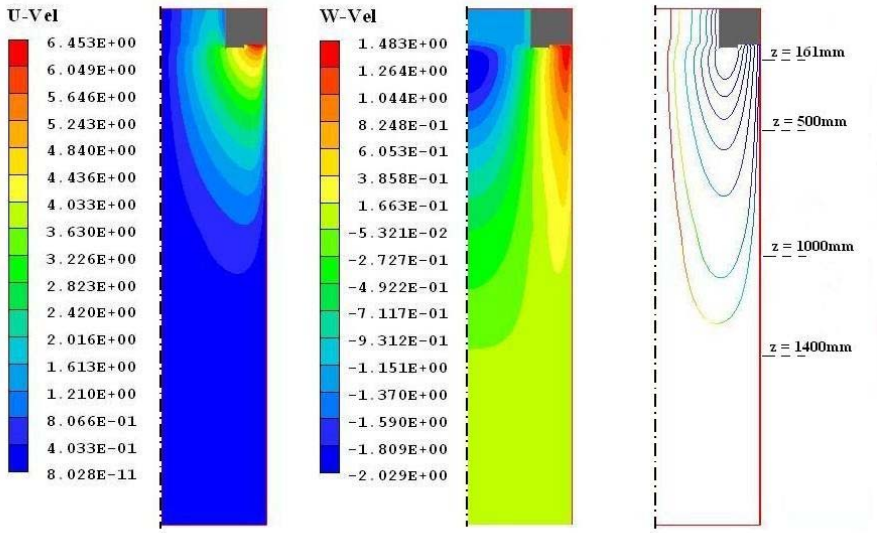

Figure 3. Velocity field for the reference case, (a) U-vel (m/s) , (b) W-vel (m/s) and (c) streamlines.

The ratio Qz/Q displayed on Fig. 5(a) starts a little over unit because there is a recirculation zone near the inlet region due the thickness of the production pipe. The decaying rate of the Qz/Q is proportional to the rate at which liquid is being transferred to the upward stream. Considering the same liquid flow rate the viscosity increase from 20cP to 100cP reduces the necessary axial length for the liquid make the U turn and causes a faster decay Qz/Q. On the other hand, keeping the same liquid viscosity of 20 cP and reducing the liquid flow rate of 116 m^3/d to 60 m^3/d also causes a change on the necessary axial length to the liquid make the U turn but not so intense as the former scenario. The decaying rate seems to have two slopes, one near the inlet and other at the end.

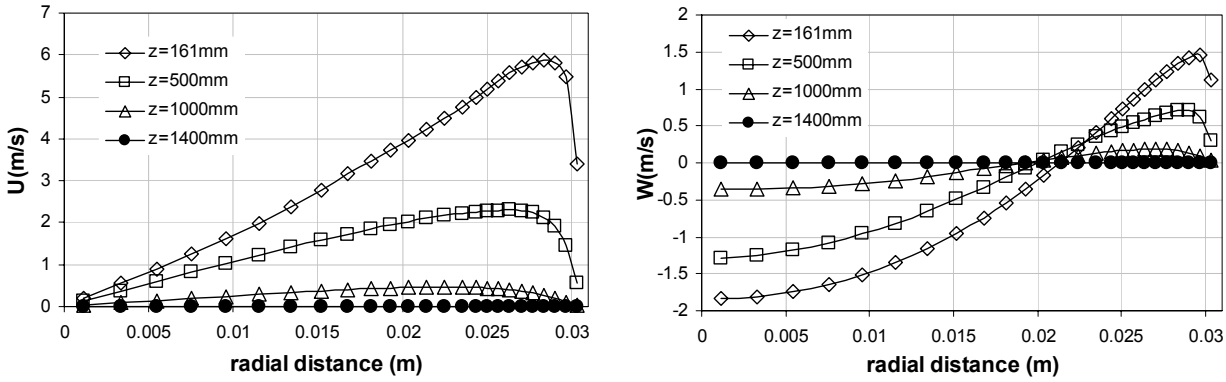

(a) (b)

Figure 4. U and W velocity profiles at different axial positions.

Table 1. Flow simulation parameters

Case number	Liquid Flow Rate, Q m^3/d	Liquid Viscosity, μ cP	Swirl Angle, α rad	Particle Diameter, dp μm
#1 (reference)	116	20	0.175	900
#2	60	20	0.175	900
#3	116	100	0.175	900

The downward liquid flow rate difference between two successive axial positions renders the radial flow rate, which transfers mass from the downward stream to the upward stream. Exploring the fact that W is null at a radial position near the outside diameter of the production pipe, Dp, then one can estimate the maximum radial velocity, VR, along any z section using the mass conservation principle:

$$dQ_z / dz = VR \cdot \pi \cdot D_p , \tag{1}$$

VR is responsible to the change of the liquid stream directions inside the device. It is shown in Fig. 5(b) for the reference case against two other cases, as described before. Since VR is deduced from a first order derivative of Qz it is more likely show noise or disturbances not seen on Qz profile. Nonetheless, VR is two orders of magnitude less than the inlet velocity, is near constant along the axial distance or exhibits a mild decay. Keeping constant the liquid flow rate of 116m^3/d and increasing the liquid viscosity from 20 cP to 100 cP one sees a increase of one and half times on the maximum radial velocity. For the case where, the liquid viscosity is kept constant in 20 cP and the liquid flow rate reduces from 116 m^3/d to 60 m^3/d, VR near the inlet is double considering the reference case but near the end of the U turn the values are the near the same, 0.07 m/s. The distinguished feature along the three cases is the progressively mass transfer along the axial distance from the downward stream to the upward stream done by VR.

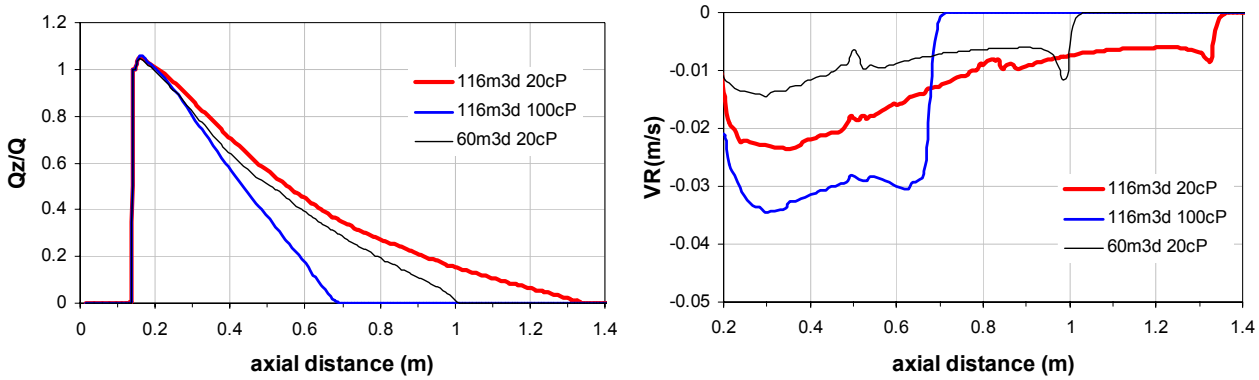

(a) (b)

Figure 5. Downward liquid flow rate ratio, Qz/Q (a) and maximum radial velocity VR (b) for 60m^3/d and 116m^3/d liquid flow rates, 20cP and 100cP liquid viscosities.

The axial and swirl velocity components exhibit a decaying rate downstream the inlet. The axial and the swirl velocities are vanishing small at nearly the same axial distance from the inlet due to the momentum coupling among U, V and W momentum equations. The decaying length, Ld, denotes the downstream distance where the velocities are vanishing small. The Ld for the cases #1, #2 and #3 listed in Tab. 1 are estimated from Fig. 5(a) as 1.3 m, 1.0m and 0.7, respectively. One observes that Ld decreases when viscosity increases or the flow rate decreases. Using the same reasoning to derive Eq. (1), the mean $\overline{VR}$ along the axial direction is estimated as:

$$Q = \overline{VR} \cdot \pi \cdot D_p \cdot L_d . \tag{2}$$

4. Capture surface of the solid particles

To understand how the separation efficiency depends on the liquid flow rate, liquid viscosity and particle size it is introduced the concept of capture surface. It is a threshold surface which divides the domain in two regions: one with separated and the other with not separated particles. Once a solid particle crosses the capture surface it can not be separated anymore but it is dragged by the upward liquid stream. A good hydrodynamic design would prevent the solids to cross the capture surface and render 100% of separation efficiency. The solids concentration, which is less than 0.1% of the inlet flow rate, is considered not disturbing the liquid flow field.

The solid particle trajectory has two directions: an axial and a radial, which in turn depends on the liquid velocity among other parameters. The liquid velocity components have distinct roles to define separation process. The axial velocity defines if a particle will be separated or not. The separation criterion is to compare the particle Stokes terminal velocity against the upward liquid velocity; it is done by the axial Stokes number (Hoffmann and Stein, 2002):

$$StkZ = (\Delta\rho \cdot d_p^{\,2} \cdot g) / (18 \cdot \mu \cdot W) , \tag{3}$$

where $\Delta\rho$ is the density difference between the solid and the liquid, d_p is the particle Sauter mean diameter, g is the gravity acceleration and μ is the liquid viscosity. Values of StkZ greater than one means that the particle terminal

velocity is greater than the liquid velocity W, therefore favorable to the particle separation. On the other hand, for 0< StkZ < 1 means the particle is being dragged by the upward liquid stream and therefore is not separated. It is expected values of 0< StkZ < 1 near the tube centerline once it is in this region where the upward liquid stream occurs.

An analysis of the liquid radial velocity component reveals that it does not define if the particle is separated or not but it has an equally important role on the separation process. It is responsible to the transport of solid particles from the outer wall toward the pipe center where they may be captured or not by the upstream liquid flow. Notice that the swirl velocity generates a centrifugal force field ($\Delta\rho\ U^2/y$) pushing the solid particles toward the outer wall. The solid particle will move inward only if the radial velocity is greater than the centrifugal force field. This scenario is likely to happen when the swirl velocity losses momentum further downstream from the inlet. The particle radial movement criterion is to compare the particle terminal velocity due to the centrifugal force field against the inward liquid velocity; it is done by the radial Stokes number:

$$StkR = (\Delta\rho \cdot d_p{}^2 \cdot U^2) / (18 \cdot \mu \cdot V \cdot y), \tag{4}$$

where y is the radial particle position. The values of StkR greater than one means that the solid particle moves outwardly due to the centrifugal force field. Complementary, 0<StkR<1 means the particle is being dragged inward.

The intersection between the surface where StkZ = 1 and the volume region where 0< StkR<1 defines the capture surface. The last define the domain region where the solids are transported inward and the former states the threshold value for the solids being separated or not. The SktZ and StkR are easily determined from the numerical data. Figure 6 displays contour plots of the StkZ, StkR and the capture surface for the reference case. The StkZ contour plot shows the area where the particle terminal velocity is smaller than the liquid upstream velocity and therefore the solid is carried by the liquid stream. Its shape is cylindrical extending along the axial direction with outer radius close to the production pipe diameter. The white colored area of the plot represent a region where liquid velocity do not have strength to carry the solid upward and therefore they are favorable to separation. The white area of the StkR contour plot shows that the solid particles do not move inward but stay put against the wall. As the swirl velocity losses momentum, weakening the centrifugal force field, the radial velocity is capable to push inward the solid particle.

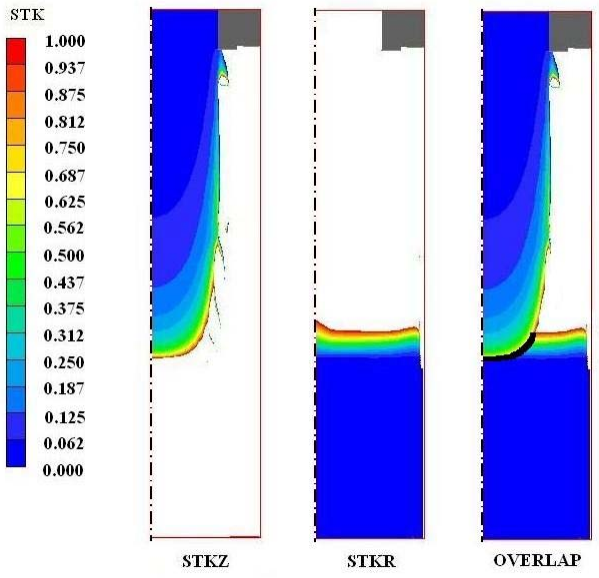

Figure 6. 0< StkZ < 1and 0<StkR < 1 regions and the capture surface (overlap).

The region of 0<StkR<1 is also cylindrical but spans from the outer wall to the tube centerline with nearly flat iso-lines. The capture surface is drawn on the 3rd contour plot. Its surface is much smaller than the surface defined by StkZ=1 because in most of its axial extension the solids can not be transported inward due to the centrifugal force field. The solid particle may cross or not the capture surface. The separation efficiency depends on the axial area extent of the capture surface, of the axial particle residence time to cross the axial distance comprised by the capture surface and of the radial velocity. It is expected that the separation efficiency will fall when there is an increase in the capture surface area or the residence time or even on the radial velocity.

5. Comparative analysis of viscosity, particle size and flow rate

This section underlines the flow mechanisms responsible to changes on the separation efficiency when the liquid viscosity, particle diameter or liquid flow rate varies. The qualitative analysis of the separation efficiency is based on the capture surface size, the residence time and the particle radial velocity (or the decaying length, Ld). The studied cases are listed in Tab. 1. Taking case #1 as reference, the analysis of the change on the liquid flow rate is drawn by comparing the outputs of cases #1 and #2, the analysis of particle diameter changes is done with case #1 alone, finally the analysis of the viscosity increase happens with case#1 against case #3. The three scenarios, in order, are depicted in Fig. 7 (a-c) as contour plots of StkR and StkZ plus the capture surface.

Figure 7(a) shows the StkZ and StkR maps and the capture surface for cases #1 and #2. As seen on the contours plots the shape and size of the capture surface for both cases are the same. More accurate measurements on the contour plots indicate the axial extent of the capture surface if of $0.89<z<0.99$ and $1.2<z<1.3$, for cases #1 and #2 respectively. Also the maximum radial velocities at the capture surface are approximately the same for cases #1 and #2, i.e. VR =0.08 m/s see Fig. 5(b). What distinguishes the two cases is axial velocity. For case #1 the downward axial velocity is almost twice the one from case #2. This is true because the downward axial velocity is proportional to the Qz/Q ratio which has almost the same slope for both cases. Since the Q from case #1 is almost twice the Q from case #2 so are the downward axial velocities. As a consequence of the increase of the downward axial velocity is a decrease of the residence time and therefore the chances to find particles crossing the capture surface decrease. It is then expected an increase on separation efficiency when the liquid flow rate increases. This behavior is in accordance with the experimentally determined separation efficiency of 94% and 80% for cases #1 and #2, respectively (Martins and Rosa, 2005).

The influence of the particle size is analyzed next. The data come from test #1 with three sizes of particles: 250μm, 900μm e 4000μm. Since there is no flow disturbance introduced by presence of the solid particles, the flow fields for the three cases are identical. The influence of the particle diameter increase shows up at the capture surface size. As seen from Fig. 7(b), by means of the capture surface, particles with 250 μm in diameter have a capture surface roughly 5 times bigger than the case with particle 900 μm in diameter and the case with particles 4000 μm in diameter shows no capture surface at all. Considering the last case, the zone of radial particle transport do not intercepts the zone with upward particle transport; therefore it is expected 100% of separation efficiency. Considering the former cases, the increase on the capture surface implies an increase on the residence time and also the odds of a particle cross the capture surface. Therefore cases with greater capture surface have smaller separation efficiency. This trend is fact confirmed by the experimental tests. The experimental separation efficiency is of 9% (correlation), 94% and 100% for the cases with particle sizes of 250 μm, 900 μm and 4000 μm, respectively (Martins and Rosa, 2005). This case reveals that the residence time depends not only on the axial downward velocity but also on the extent of the capture surface, which, by its turn, depend on the particle size.

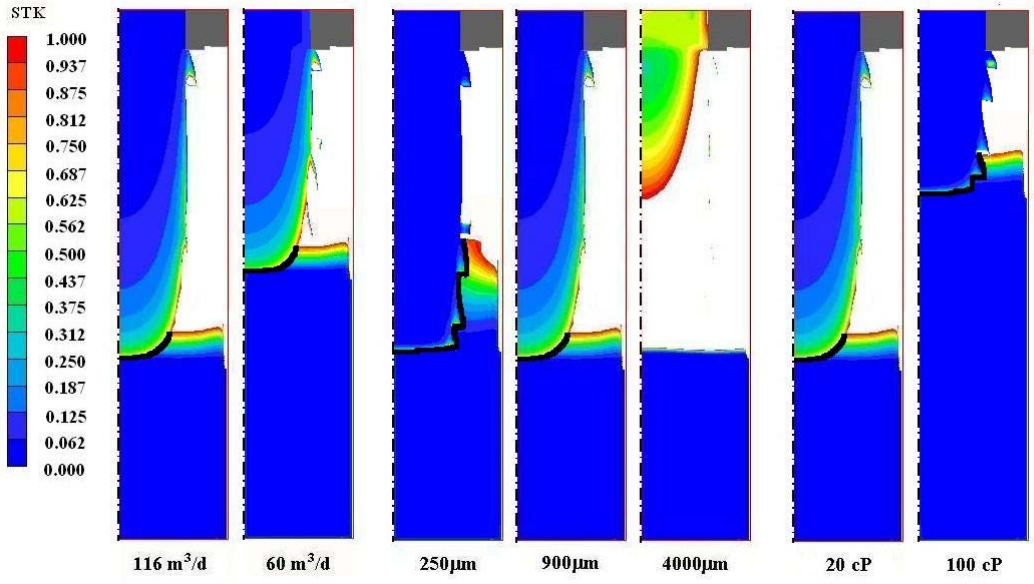

(a) (b) (c)

Figure 7. StkZ < 1and StkR < 1regions and capture surface for different viscosities, flow rate and particle sizes.

The effect of increasing the liquid viscosity is now analyzed. The selected cases are #1 and #3 from Tab. 1, which have the same flow rate but liquid viscosities of 20cP and 100cP. The capture surface is shown in Fig. 7(c). Measurements on the contour plot indicate that the axial extent of the capture surface is of $1.20<Z<1.32$ and $0.53<Z<0.70$ corresponding to the cases of 20 cP and 100 cp respectively. Also the maximum radial velocity, VR, for the 20 cP case is 1.5 times smaller than the one observed for 100 cP, see Fig. 5(b). Summarizing, the case with 20cP has a smaller capture surface, which translates into a smaller residence time and also a smaller maximum radial velocity when compared against the case with 100 cP. These two factors are favorable to better separation efficiency in case with 20 cP than the one with 100 cP. This trend is also seen on the experimentally determined separation efficiency of 94% and 9% for the cases with 20cP and 100cP respectively (Martins and Rosa, 2005).

6. Conclusions

Some aspects of the flow mechanics of the separation process inside the swirl-tubes were disclosed. The flow field is three dimensional with axis-symmetry but its main characteristics are defined by the decay length, Ld, with the aid of the inlet flow rate and the geometrical parameters: the swirl angle and the diameters of the production pipe and external pipe. The decay length decreases as the liquid viscosity increases or the liquid flow rate decreases, it is sensitive to the flow inertia. The axial and swirl velocities components decay downstream the inlet and have a decay rate proportional to Ld. The maximum radial liquid velocity transfers mass from the downward stream to the upward stream. Considering the flow area of the upward stream defined by the production pipe diameter, then the VR is estimated by Eq. (1).

The Stokes numbers are defined along the axial and radial direction with the aid of the liquid and the Stokes particle terminal velocity. It is introduced the concept of capture surface based on the Stokes number. The later is a threshold surface, if a solid particle crosses the surface it will be no longer separated but carried by the upward liquid stream. These concepts helped to analyze the effects of increasing liquid flow rate, particle diameter and liquid viscosity on the separation efficiency. The increase on the liquid flow rate decreases the particle residence time, reduces the chances of a particle intercept the capture surface and thus leads to an increase on the separation efficiency. The increase on the particle diameter reduces or even eliminates the capture surface it thus decreases the residence time and improves the separation efficiency. Finally, the increase on the liquid viscosity causes an increase on the residence time and also on the radial velocity. These two features act on the same direction to lessen the separation efficiency. Increasing the residence time and the radial velocity increases the chances to have a solid particle crossing the capture surface.

7. Acknowledgements

The authors J.A. Martins and E.S. Rosa would like to thank to Petrobras to support this research under the contract number 650.2.303.03.3 and also thanks to MSc. Robson de Oliveira Souza, Eng. Nelson Shiratori and Dr. Waldir Estevan from Petrobras for the useful suggestions and encouragement.

8. References

Hoffmann, A.C. and Stein, L.E., 2002, “Gas Cyclones and Swirl Tubes: Principles, Design and Operation”, Springer-Verlag, 334.

Martins, J.A., Rosa, E.S., 2005, “Experimental Analysis of Swirl Tubes as Downhole Desander Device”, Proceedings of the 9th Latin American and Caribbean Petroleum Engineering Conference, Rio de Janeiro, Brazil.

Patankar, S.V., 1980, “Numerical Heat Transfer and Fluid Flow”, Hemisphere, Washington, E.U.A.

POLIS, 2005, “The PHOENICS On-Line Information System”, http://www.cham.co.uk/.

9. Responsibility notice

The authors J.A. Martins and E.S. Rosa are the only responsible for the printed material included in this paper.